ARTICLE

Theoretical and Experimental Study of Photophysical Characteristics between Poly(9,9-dioctylfluorene) and Poly(9,9-dioctylfluorene-co-benzothiadiazole)

Li-quan Zhang[a,c], Ying-hui Wang[a,b*], Ning Sui[a], Zhi-hui Kang[a], Tian-hao Huang[a], Yu-guang Ma[b], Han-zhuang Zhang[a*]

a. Femtosecond laser laboratory, College of Physics, Jilin University, Changchun 130012, China
b. State Key Laboratory of Supramolecular Structure and Materials, Jilin University, Changchun 130012, China
c. Teaching Center of Basic Courses, Heping Campus, Jilin University, Changchun 130062, China

(Dated: Received on March 30, 2013; Accepted on May 13, 2013)

The photo-physical characteristics of semiconductor polymer are systematically studied through comparing poly (9,9-dioctylfluorene) (PFO) and poly (9,9-dioctylfluorene-co-benzothiadiazole) (F8BT). The quantum chemical calculation shows that the introduction of benzothiadiazole unit facilitates the intrachain charge transfer (ICT) and modulates the electronic transition mechanism of polymer. The transient absorption measurement exhibits that intrachain exciton relaxation is dominant in the decay of excited PFO in a monodisperse system and intrachain exciton interaction could appear at high excitation intensity. In F8BT solution, the ICT state exists and participates in the relaxation of excited state. The relaxation processes of PFO and F8BT in the condensed phase both accelerate and show obvious exciton-exciton annihilation behavior at high excitation intensity. At the same excitation intensity, the mean lifetime of F8BT is longer than that of PFO, which may be assigned to the excellent delocalization of charge.

Key words: Conjugated polymer, Transient absorption spectroscopy, Intrachain charge transfer

I. INTRODUCTION

In the steadily growing field of organic field effect transistor (FET) [1] and organic light emitting diode (LED) [2], several types of polymer systems and device architectures have emerged as attractive means to improve the performance of the devices. In order to obtain the polymer with high performance, the photophysical characteristics, such as the transition mechanism, exciton generation and carrier diffusion, are gradually modulated through molecular engineering [3] and a large number of conjugated polymers are synthesized. Polyfluorene polymer is one of the excellent blue light polymers [4]. After introduction of alkyl side chains, this semiconductor polymer (PFO) exhibits good solubility, which is beneficial to the application in polymer LED [5]. In order to modulate the color of emission band and increase the mobility of carriers, one particular type of promising structure that has been explored with success is characterized by the presence of units with different electron affinities, forming a type of donor-acceptor (D-A) system, which may favor intra- and inter-chain exciton transport. Therefore, many conjugated units with different electron affinities, involving quinoline [6], thiophene [7], pyridazine and benzothiadiazole [9], *etc.*, have been used, so as to improve the photo-physical properties of conjugated polymer. F8BT is one of the important derivatives based on poly (9,9-dioctylfluorene) polymer, and has been extensively investigated in the field of organic optoelectronic applications [9]. In comparison with PFO, F8BT exhibits excellent delocalization character of charge and its color of emission band has been modulated after the introduction of benzothiadiazole unit. In order to further expatiate the difference between the A type conjugated polymers and A-D type conjugated polymers, it is necessary to compare their basic transition and relaxation mechanisms in the monodisperse system and aggregation state, which helps to understand the pristine photophyscial behavior of conjugated polymer.

In this work, the electronic transition mechanisms of PFO and F8BT have been compared through quantum chemical calculation and their photoexcitation dynamics have been probed by using femtosecond transient absorption (TA) technique. Their decay behavior in

*Authors to whom correspondence should be addressed. E-mail: wangyinghuijlu@yahoo.cn, zhanghz@jlu.edu.cn, Tel.: +86-431-85167378, FAX: +86-431-85166112

the monodisperse system and condensed phase are both compared, which helps to understand the influence of interchain interaction in the exciton relaxation of conjugated polymer.

II. EXPERIMENTS

A. Materials

The chemicals used were all purchased from Derthon Technology, without further purification. The polymers dissolved in chlorobenzene (CB) solvent with concentration of 100 μg/mL so as to exclude the influence of interchain species in the relaxation process of excited state [10]. The solution samples were encapsulated in 1 mm thick quartz cell. All films were obtained through spin coating from CB solution with concentration of 10 mg/mL.

B. Experimental

Steady-state absorption measurements were carried out using a UV-Vis spectrophotometer (Purkinje, TU-1810PC). Photoluminescence (PL) spectra were recorded by a fiber optic spectrometer (Ocean Optics, USB4000) with excitation pulse at 400 nm. For the optical investigations, a mode-lock Ti:sapphire femtosecond laser system (Coherent) was employed. It offers 2.0 mJ, 130 fs pulses at 800 nm with a repetition rate of 1 kHz. Femtosecond TA measurements have been performed using two-color pump-probe technique [11]. The output of femtosecond laser beam was split into two parts: the major one was frequency-doubled by a 1 mm thick BBO crystal to generate 400 nm pulses which will be used as the pump beam, while the minor one was focused into a 5 mm quartz cell filled with water to generate a white light continuum as the probe beam. The pump beam was continuously chopped by the optical chopper and finally focused into the sample cell after passing through an optical delay line, while the probe beam was also focused into the sample to overlap with the pump beam before it traveled through a monochromator. The time-dependent transmittance change was detected by a photomultiplier tube (Zolix, PMTH-S1-CR131A) connected to the lock-in amplifier (SR830, DSP). All the measurements were carried out at room temperature.

C. Computational methods

All the quantum chemical calculations were done with Gaussian 09 program package [12]. The electronic properties of PFO and F8BT with two repeat units, and the corresponding ground and excited state geometries were calculated at the density functional theory (DFT) level

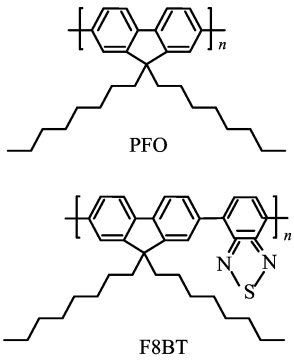

FIG. 1 The molecular structures of PFO and F8BT.

using the B3LYP functional and 6-31G basis set [13]. The influence of peripheral carbon chains was believed to be small [14] enough for such chains neglected in the quantum chemical calculations. Electronic transition in optical absorption was computed with time-dependent DFT (TD-DFT) [15], the long range corrected CAM-B3LYP functional [16], and 6-31G(d) basis set. All the electronic properties and geometries were calculated by assuming the oligomer of PFO and F8BT with two repeat units as isolated oligomers in vacuum.

III. RESULTS AND DISCUSSION

The molecular structures of PFO and F8BT are shown in Fig.1, where a benzothiadiazole group is introduced in the repeat unit of F8BT in comparison with PFO. The steady-state absorption and PL spectra of PFO and F8BT in the CB solution and the condensed phase are shown in Fig.2. The absorption spectrum of PFO consists of one absorption peak at 390.5 nm (CB solution) and 385 nm (solid film), with similar spectral shape. Meanwhile, the band edge apparently red shifts from 427 nm (CB solution) to 457 nm (solid film). The emission spectrum of PFO in CB solution consists of three peaks (420.5, 443.3, and 480.8 nm) and a shoulder (508 nm). In the film, although these fine emission peaks all exist, they are red-shifted to 438.5, 467.5, 498.7, and 531 nm, respectively. The band gap of PFO could be estimated from the intersection point between the first absorption band and the first emission peak, which is ∼3.02 eV (CB solution) and 2.92 eV (solid film), respectively. The Stokes shift, given by the frequency difference between the emission maximum and the first absorption peak, is ∼1827 cm^{-1} (CB solution) and 3168 cm^{-1} (solid film), respectively, and it apparently broadens after aggregation. For F8BT, its absorption consists of two absorption bands, and its first absorption band is at ∼454.5 nm in CB solution and at ∼461 nm in aggregation film. Its PL peak is at ∼538 nm in CB solution and at ∼550 nm in film. Unlike PFO, the PL spectrum of F8BT shows a good enantiomorphous feature in comparison with its first absorption

DOI:10.1063/1674-0068/26/04/387-392

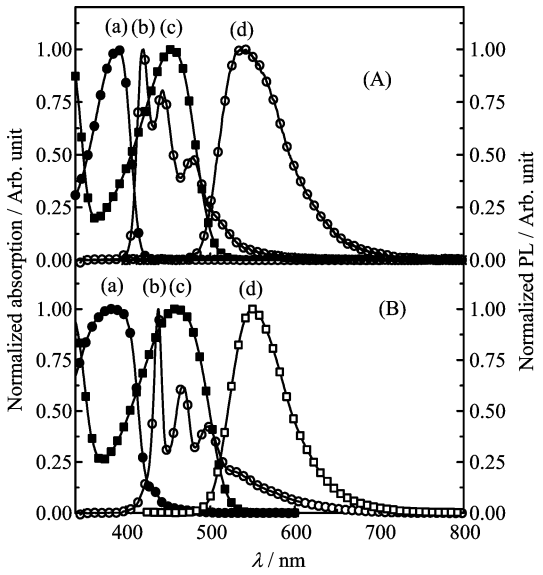

FIG. 2 Normalized absorption and PL spectra of PFO ((a) and (b)) and F8BT ((c) and (d)) in the soltuion (A) and the film (B).

band, no matter F8BT in the solution or solid film. The bandgap of F8BT also decreases from ∼2.49 eV (CB solution) to 2.43 eV (solid film) due to aggregation, and the Stokes shift increases from ∼3415 cm^{-1} (CB solution) to ∼3510 cm^{-1} (solid film), which has the same tendency as that of PFO. After the introduction of benzothiadiazole group in one repeat unit, the bandgap of conjugated polymer becomes narrow and the absorption band edge apparently red shifts, due to the extension of π-conjugated system.

The geometry of the oligomers (PFO and F8BT) containing two repeating units are optimized by B3LYP/6-31G, and shown in Fig.3 (a) and (b), respectively. For PFO, the fluorene units show a good coplanarity. However, there is a little torsion between them. For F8BT, its repeating units also exhibit a good coplanarity, and the twist also exists between the repeating units. In addition, the LUMO and HOMO of PFO oligomer are also shown in Fig.3(a). Both of them are localized in the fluorene moiety, indicating that no obvious intrachain charge transfer (ICT) would occur in the repeat units after photoexcitation. For F8BT, its HOMO is distributed over the whole oligomer, while its LUMO is mainly localized in the benzothiadiazole unit. Apparently, the ICT would occur after photoexcitation, indicating that ICT should participate in the electronic transition. Moreover, the dipole moment was enhanced obviously from 0.3118 Debye (PFO) to 3.5031 Debye (F8BT), and the reason may be assigned to the ICT character. Meanwhile, the simulated absorption spectra of PFO and F8BT oligomer with TD-DFT/6-31G are presented in Fig.3 (c) and (d), and the contributions of the frontier molecular orbitals to the electronic transitions were analyzed. Similar to the experimental data, the simulated absorption spectra (SAS) of F8BT shows a red shift in comparison with that of PFO. The main absorption band of PFO may be ascribed to $S_0 \rightarrow S_1$ transition, which is mainly composed of H→L transition. For F8BT, the $S_0 \rightarrow S_1$ and $S_0 \rightarrow S_{10}$ transitions may be dominant in the electronic transition and responsible for two main bands in the SAS. The $S_0 \rightarrow S_1$ transition is mainly assigned to the H→L (ICT) transition, indicating that the ICT would influence the absorption spectrum, while the $S_0 \rightarrow S_{10}$ transition is mainly attributed to the H→L+2 transition. The simulated absorption spectra of PFO and F8BT surely have some difference in comparison with the experimental data, since the number of repeat units is not enough and the calculated oligomers is assumed to be in vacuum.

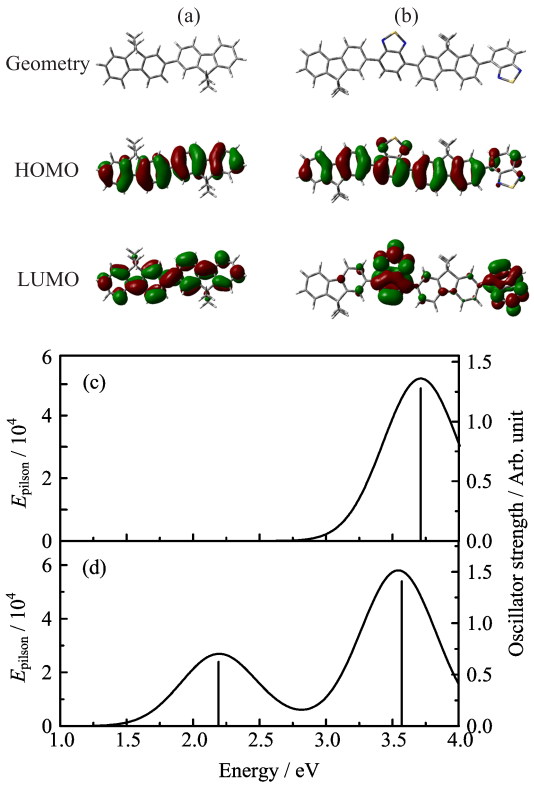

FIG. 3 Electronic ground state optimized geometry and the charge density distribution (HOMO and LUMO) for (a) PFO and (b) F8BT with two structure units, simulated absorption spectra of (c) PFO and (d) F8BT oligomers with two repeat units.

The time-dependent TA spectra of the PFO and F8BT in the monodisperse system with excitation wavelength of 400 nm are reported in this work. As seen in Fig.4(a), the TA spectra of PFO consist of a positive spectral feature and two broad negative bands. The positive one is at 400 nm, which may be assigned to the ground state photo-blenching ($GSPB_1$) band, according to its absorption absorption spectrum. The negative spectral bands are attributed to the fingerprint of

DOI:10.1063/1674-0068/26/04/387-392

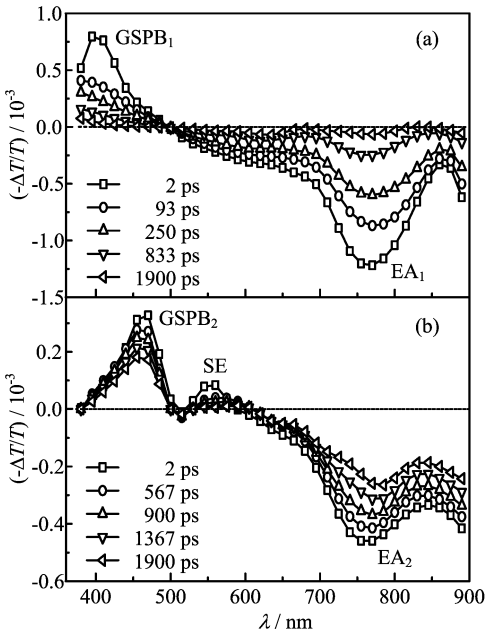

FIG. 4 Time-dependent TA spectra of (a) PFO and (b) F8BT in CB solution at excitation intensity of 48 μJ/cm^2 from ∼1 ps to ∼2 ns in the visible and the near IR spectral regions.

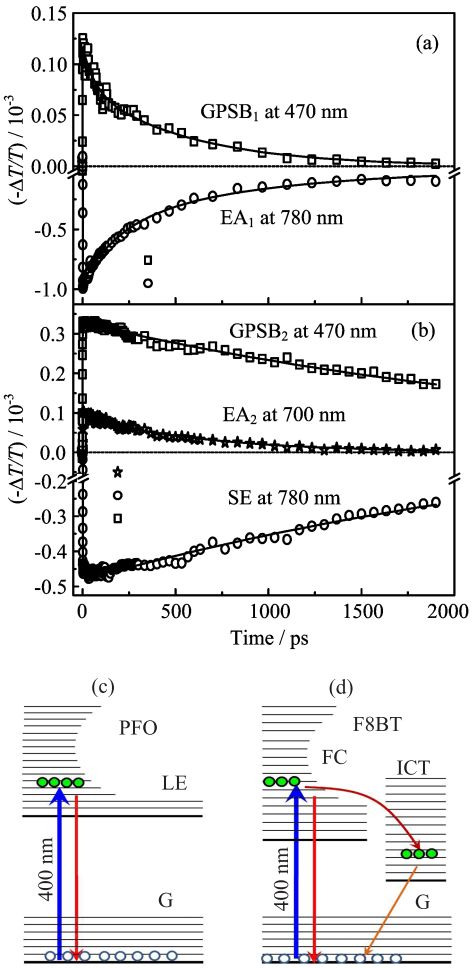

FIG. 5 (a) TA curves of PFO in solution at 470 and 780 nm. (b) TA curves of F8BT in solution at 470, 700, and 780 nm. Sketch of the primary photophysical events occurring upon photoexcitation (c) PFO and (d) F8BT and the fitted lines are shown by the solid lines. LE: localized exciton state, FC: Frank Condon state, ICT: intramolecular charge transfer state, G: ground state.

excited state (EA_1).

The TA curves of $GSPB_1$ and EA_1 at 470 and 780 nm are shown in Fig.5(a), and both of them gradually decrease to the baseline with time. It is noted that they display the similar temporal decay. This suggests that they should be related to the transition from the localized exciton state, as depicted in Fig.4(a). The dynamics were fitted by a biexponential function and the fitted results are shown in Fig.5(a) with solid lines. The TA spectra of F8BT are composed of two positive bands and two negative bands. The positive spectral bands at 450 and 550 nm are assigned to the $GSPB_2$, which is the groun state photo-blenching band in F8BT, and stimulated emission (SE), since their positions are consistent with those of absorption and emission peaks. The negative bands should also correspond to the absorption of excited state (EA_2). Thus, the $GSPB_2$, SE, and EA_2 curves of F8BT at 470, 560, and 780 nm, respectively, are exhibited in Fig.5(b). Their different temporal decay reflects that different species that come from different energy states are being monitored. Therefore, the dynamics were fitted by a multi-exponential function. The fitted results have been shown in Fig.5(b) with solid lines. It is found that the lifetime of $GSPB_2$ and SE are ∼3.0 and ∼3.5 ns, respectively. Meanwhile, the EA_2 curve exhibits a rising behavior in the initial dynamic process with lifetime of 25 ps, showing that an intermediate state appears in the relaxation process after photoexcitation. The relaxation process of excited F8BT is much more complex in comparison with that of PFO and the intermediate state may be assigned to the interconversion originating from the ICT. These results are consistent with the calculated results as seen in Fig.3. For F8BT, an intermediate state corresponding to ICT state could participate in the relaxation process of excited F8BT and compete with the SE, as shown in Fig.5(d). The intrachain charge transfer is an important dynamic process in the F8BT polymer and still exists in its derivatives [17]. Since this intrachain charge transfer mainly occurs on the main chain of conjugated polymer, it would be insensitive to the structure change of the side chain [17].

In order to further compare the photoexcitation dynamics of PFO and F8BT, the excitation intensity-dependent TA curves at 780 nm are offered, as seen in Fig.6, and all of them are fitted with multi-exponential function. Meanwhile, the initial amplitude of TA curves at different excitation intensities are also presented in

DOI:10.1063/1674-0068/26/04/387-392

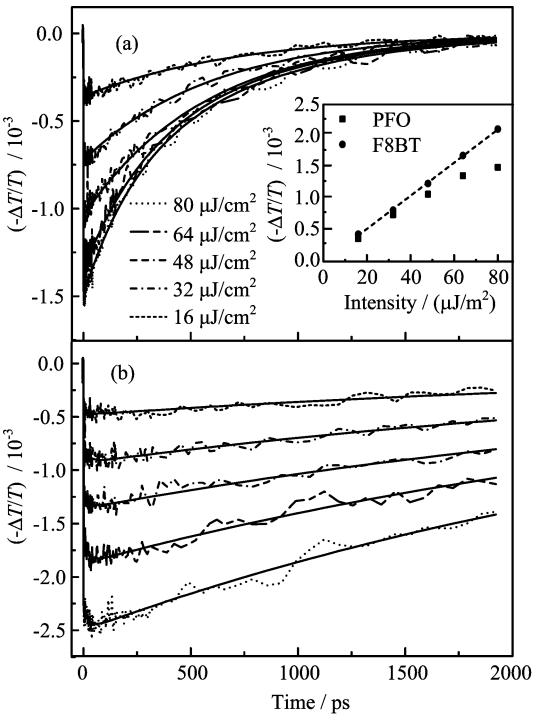

FIG. 6 Intensity-dependent TA curves of (a) PFO at 780 nm and (b) F8BT at 700 nm in solution and the fitted lines are shown by the solid lines. Inset: the amplitude of PFO and F8BT at initial 0.4 ps after photo-excitation.

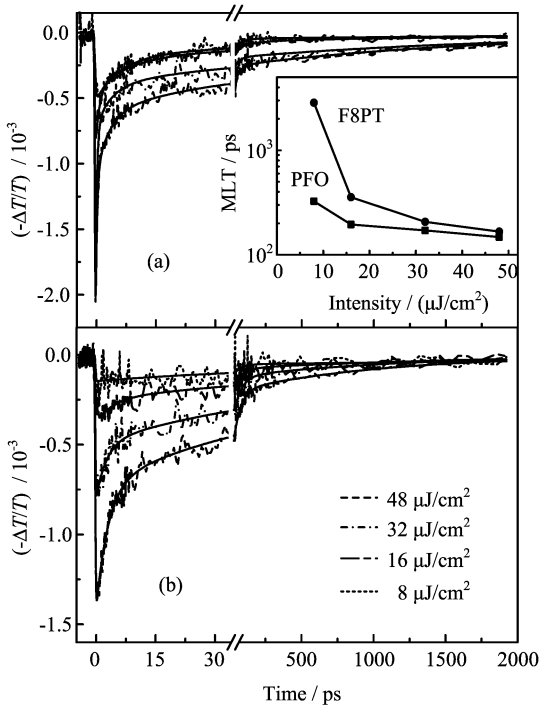

FIG. 7 Intensity-dependent TA curves of (a) PFO and (b) F8BT in film and the fitted lines are shown by the solid lines. Inset: the mean lifetime (MLT) of PFO and F8BT films *vs.* excitation intensity.

the inset of Fig.6. The fitted results show that the mean lifetime of PFO gradually decreases from 716 ps to 495 ps when the excitation intensity is enhanced from 16 μJ/cm^2 to 80 μJ/cm^2. It suggests that localized intrachain exciton relaxation is dominant in the decay process of excited PFO and that they could interact with each other, accelerating the relaxation process after photoexcitation. However, the rising time and decay time of F8BT are ∼24 ps and ∼3.4 ns, respectively, and both of them are almost independent of the excitation intensity. It indicates that the intrachain exciton could be well delocalized in the main chain and this could not give rise to the interaction between intrachain exciton. Therefore, the relaxation process of F8BT is almost invariable when the excitation intensity is lower than 80 μJ/cm^2. Moreover, the initial signal intensity at 0.4 ps under different excitation intensities at 400 nm is measured, as seen in the inset of Fig.6. Apparently, the initial signal intensity of F8BT linearly enhances with the increase of excitation intensity. On the contrary, those of PFO show nonlinearly increase behavior as the excitation intensity increases. These different enhancement behaviors of PFO and F8BT again indicate that the intrachain exciton interaction could not exist in the F8BT, due to its excellent ICT character.

Next, the intensity-dependent TA curves of PFO and F8BT in solid films are also presented in Fig.7 and all of them show obvious relaxation behavior without a rising behavior, due to the interchain interaction in condensed phase. Apparently, the ICT process disappears under the interchain interaction. In addition, an intensity-dependent fast dynamic process appears in the TA curves at high excitation intensity, which make the photoexcitation dynamics become complicate, and its percentage gradually increases with the enhancement of excitation intensity. This indicates that this fast dynamic process could be assigned to the exciton-exciton annihilation (EEA), which could accelerate the annihilation of exciton when its concentration is high. Moreover, the intensity-dependent EEA also exists in the relaxation of excited F8BT at high excitation intensity, as seen in Fig.7(b). However, the mean lifetimes of F8BT should be longer than that of PFO, since the ICT character originated from the delocalization of π-conjugated system facilitates the migration of exciton in the aggregation of polymer.

IV. CONCLUSION

The photo-physical characteristics of PFO and F8BT are systematically investigated through experimental and theoretical approaches. The quantum chemical calculation exhibits the electronic transition mechanisms of PFO and F8BT and simulates their absorption spectra. The results confirm that delocalization of intrachain charge occurs in F8BT in a monodisperse sys-

DOI:10.1063/1674-0068/26/04/387-392

tem. Femtosecond transient absorption (TA) measurement shows that localized intrachain exciton is dominant in the relaxation of excited PFO, and an intermediate state, which is closed to delocalization of intrachain charge, appears in the relaxation of excited F8BT. In addition, the intensity-dependent TA curves of PFO and F8BT in a monodisperse system suggest that although interchain exciton interaction could influence the relaxation behavior of PFO, it could not influence that of excited F8BT. The intensity-dependent TA curves of PFO and F8BT in solid film exhibit that the intermediate state could disappear in the relaxation process of F8BT. Both of them could show intensity-dependent exciton-exciton annihilation process at high excitation intensity in condensed phase, and the relaxation lifetime of F8BT should be longer than that of PFO due to its good ICT character.

V. ACKNOWLEDGMENTS

This work was supported by the National Natural Science Foundation of China (No.21103161 and No.11274142), the Jilin Province Natural Science Foundation of China (No.20070512), the National Found for Fostering Talents of Basic Science (No.J1103202), and the China Postdoctoral Science Foundation (No.2011M500927).

[1] H. Sirringhaus, P. J. Brown, R. H. Friend, M. M. Nielsen, K. Bechgaard, B. M. W. Langeveld-Voss, A. J. H. Spiering, R. A. J. Janssen, E. W. Meijer, P. Herwig, and D. M. de Leeuw, Nature **401**, 685 (1999).
[2] R. H. Friend, R. W. Gymer, A. B. Holmes, J. H. Burroughes, R. N. Marks, C. Taliani, D. D. C. Bradley, D. A. Dos Santos, J. L. Bredas, M. Logdlund, and W. R. Salaneck, Nature **397**, 121 (1999).
[3] T. M. Clarke and J. R. Durrant, Chem. Rev. **110**, 6736 (2010).
[4] V. N. Bliznyuk, S. A. Carter, J. C. Scott, G. Klärner, R. D. Miller, and D. C. Miller, Macromolecules **32**, 361 (1999).
[5] S. Y. Cho, A. C. Grimsdale, D. J. Jones, S. E. Watkins, and A. B. Holmes, J. Am. Chem. Soc. **129**, 11910 (2007).
[6] A. P. Kulkarni, Y. Zhu, A. Babel, P. T. Wu, and S. A. Jenekhe, Chem. Mater. **20**, 4212 (2008).
[7] V. R. Donuru, G. K. Vegesna, S. Velayudham, S. Green, and H. Y. Liu, Chem. Mater. **21**, 2130 (2009).
[8] Y. S. Park, D. Kim, H. Lee, and B. Moon, Org. Lett. **8**, 4699 (2006).
[9] J. S. Kim, L. Lu, P. Sreearunothai, A. Seeley, K. H. Yim, A. Petrozza, C. E. Murphy, D. Beljonne, J. Cornil, and R. H. Friend, J. Am. Chem. Soc. **130**, 13120 (2008).
[10] N. Banerji, S. Cowan, M. Leclerc, E. Vauthey, and A. J. Heeger, J. Am. Chem. Soc. **132**, 17459 (2010).
[11] Y. H. Wang, J. Q. Hou, Z. H. Kang, L. J. Gong, T. H. Huang, L. L. Qu, Y. G. Ma, R. Lu, and H. Z. Zhang, Chem. Phys. Lett. **566**, 17 (2013)
[12] M. J. Frisch, G. W. Trucks, H. B. Schlegel, G. E. Scuseria, M. A. Robb, J. R. Cheeseman, G. Scalmani, V. Barone, B. Mennacci, G. A. Peterson, H. Nakatsuji, M. Caricato, X. Li, H. P. Hratchian, A. F. Izmaylov, J. Bloino, G. Zheng, J. L. Sonnenberg, M. Hada, M. Ehara, K. Toyota, R. Fukuda, J. Hasegawa, M. Ishida, T. Nakajima, Y. Honda, O. Kitao, H. Nakai, T. Vreven, J. A. Jr. Montgomery, J. E. Peralta, F. Ogliaro, M. Bearpark, J. J. Heyd, E. Brothers, K. N. Kudin, V. N. Staroverov, R. Kobayashi, J. Normand, K. Raghavachari, A. Rendell, J. C. Burant, S. S. Iyengar, J. Tomasi, M. Cossi, N. Rega, J. M. Millam, M. Klene, J. E. Knox, J. B. Cross, V. Bakken, C. Adamo, J. Jaramillo, R. Gomperts, R. E. Stratmann, O. Yazyev, A. J. Austin, R. Cammi, C. Pomelli, J. W. Ochterski, R. L. Martin, K. Morokuma, V. G. Zakrzewski, G. A. Voth, P. Salvador, J. J. Dannenberg, S. Dapprich, A. D. Daniels, O. Farkas, J. B. Foresman, J. V. Ortiz, J. Cioslowski, and D. J. Fox, *Gaussian 09, Revision A.02*, Wallingford CT: Gassian, Inc., (2009).
[13] C. Lee, W. Yang, and R. G. Parr, Phys. Rev. B **37**, 785 (1988).
[14] S. Sergeyev, E. Pouzet, O. Debever, J. Levin, J. Gierschner, J. Cornil, R. G. Aspe, and Y. H. Geerts, J. Mater. Chem. **17**, 1777 (2007).
[15] E. K. U. Gross and W. Kohn, Phys. Rev. Lett. **55**, 2850 (1985).
[16] T. Yanai, D. Tew, and N. Handy, Chem. Phys. Lett. **393**, 51 (2004).
[17] Y. H. Wang, L. J. Gong, W. Y. Dong, P. Lu, Z. H. Kang, T. H. Huang, Y. G. Ma, and H. Z. Zhang, J. Polym. Sci. Pol. Phys. **51**, 992 (2013).

DOI:10.1063/1674-0068/26/04/387-392